

# Room Temperature Acoustic Transducers For High-Temperature Thermometry

D. C. Ripple, W. E. Murdock, G. F. Strouse, K. A. Gillis, and M. R. Moldover

*Sensor Science Division, National Institute of Standards and Technology,  
100 Bureau Drive, Gaithersburg MD, USA*

**Abstract.** We have successfully conducted highly-accurate, primary acoustic thermometry at 600 K using a sound source and a sound detector located outside the thermostat, at room temperature. We describe the source, the detector, and the ducts that connected them to our cavity resonator. This transducer system preserved the purity of the argon gas, generated small, predictable perturbations to the acoustic resonance frequencies, and can be used well above 600 K.

**Keywords:** acoustic thermometer, acoustic transducers, high temperature, primary thermometry, speed of sound

## INTRODUCTION

Since 1999, five acoustic thermometers have been used to measure  $T-T_{90}$ , the difference between the thermodynamic temperature  $T$  and the International Temperatures Scale of 1990. [1] These measurements spanned the range 7 K to 552 K and each used either a spherical or a quasi-spherical, cavity resonator with small, capacitive, electro-acoustic transducers embedded within the cavity's wall. Because of their small size and high mechanical impedance, these embedded transducers generated small, predictable perturbations to the acoustic resonance frequencies of the gas-filled cavities. For our previous measurements of  $T-T_{90}$ , we constructed embedded transducers from materials that did not contaminate the thermometric gas, even at 552 K. [2] However, at higher temperatures, where it is impossible to install a preamplifier near the detector transducer, the triaxial cable connecting the detector to the room-temperature preamplifier caused significant difficulties. Erratic fluctuations in the resistance of the alumina insulators coupled with the high voltage bias across these insulators caused unacceptably high noise. Additionally, the signal strength dropped appreciably at elevated temperatures.

To eliminate the problems caused by cables, we developed the alternative transducer system sketched in Fig. 1. This system uses two ducts; one to transport sound from an acoustic source at room temperature to the cavity resonator at high temperature and a second to return sound from the cavity to a detector at room temperature. Here, we list the acoustic system's design objectives, explain how we retrofit the acoustic thermometer, and report the system's performance.

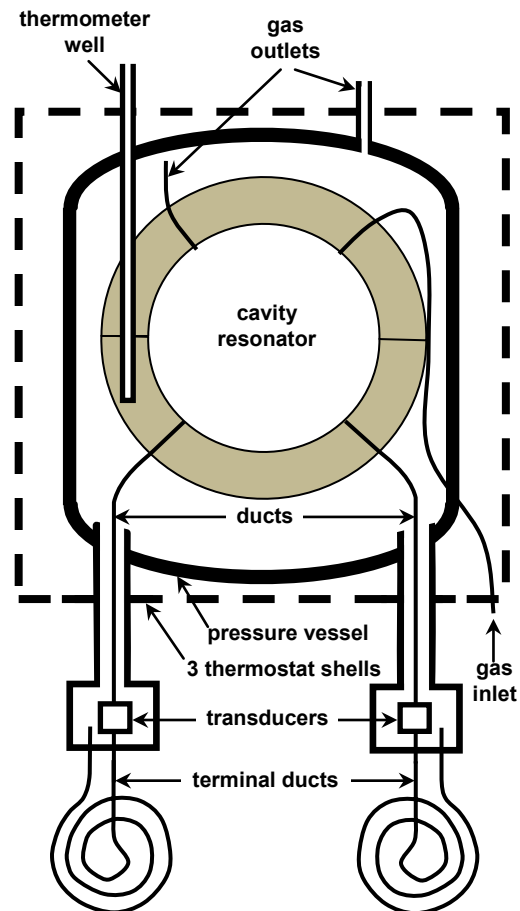


**Figure 1.** Transducer system. The transducers are at room temperature outside the 3 thermostatted shells; however, they are inside extensions of the pressure vessel.

## OBJECTIVES AND CONCEPTS

Our goal is to conduct accurate, primary acoustic thermometry at temperatures  $T \geq 600$  K using NIST's existing 3-liter-cavity acoustic thermometer. [2] This goal led to the following design objectives for the system {ducts + transducers}:

- does not contaminate thermometric gas,
- has signal-to-noise ratio  $> 1000$  throughout the range 50 kPa to 400 kPa,
- perturbs the  $(0,n)$  radial modes of the gas-filled cavity by an amount less than 1 mK equivalent,
- does not mechanically excite resonances in the cavity's walls, supports, or appendages, near the frequencies of the  $(0,n)$  modes,
- has negligible electrical and acoustic cross-talk between acoustic source and acoustic detector,
- does not degrade the thermostating of the cavity,
- generates a detector-voltage proportional to source voltage so that the shapes of the  $(0,n)$  resonances are not distorted at the  $\sim 0.1\%$  level,
- adds perturbations to the seven components of the  $(3,1)$  non-radial mode that are so small that no component overlaps the  $(0,2)$  radial mode.

We achieved the listed objectives using the design concepts sketched in Fig. 1. The source and detector transducers were located inside separate housings attached to extensions of the pressure vessel. Each housing was at room temperature (outside the furnace). Ducts of length  $l_{\text{trans-cavity}}$  transported sound between the transducers and the cavity resonator. These ducts did not terminate at the transducers. Instead, each duct had an extension of length  $l_{\text{terminal}}$  that passed through the wall of the transducer housing to a coil at room temperature and then back into the housing where it terminated with an open end. (See Table 1 for relevant dimensions.)

Design of the {ducts + transducer} system requires optimization between high signal to noise ratio (favoring short, large-diameter ducts and large transducers) and small perturbations (favoring long, small-diameter ducts and small transducers). To gain insight into the design trade-offs, we consider an idealized acoustic thermometer filled with a low-density noble gas with the Prandtl number  $Pr \approx 0.66$ , the heat-capacity ratio  $\gamma = 5/3$ , and the quantity  $\xi \equiv 1 + Pr^{1/2} - \gamma \approx 0.15$ . This thermometer is composed of a spherical cavity with the radius  $a_{\text{cavity}}$  joined to two infinitely-long, circular ducts. The source duct has the radius  $a_s$  and the detector duct has the radius  $a_{\text{det}}$  and both radii are much larger than the viscous and thermal penetration lengths,  $\delta_v$  and  $\delta_T$ . The very small acoustic source and detector are located at a tee in their ducts at distances  $l_s$  and  $l_{\text{det}}$  from the cavity-duct joints.

Following Gillis *et al.* [3], we estimate the ratios of the acoustic pressures at the source, cavity, and detector in the limit where the acoustic impedances of the ducts are much larger than the acoustic impedance of the cavity:

$$\left| \frac{p_{\text{cavity}}}{p_s} \right| = \frac{Q_{(0,n)}}{z_{(0,n)}} \frac{a_s^2}{a_{\text{cavity}}^2} e^{-(\alpha l)_s} \quad ; \quad \left| \frac{p_{\text{det}}}{p_{\text{cavity}}} \right| = e^{-(\alpha l)_{\text{det}}} \quad . \quad (1)$$

In Eq. (1),  $z_{(0,n)}$  is the eigenvalue of the  $(0,n)$  mode of the cavity and  $\alpha^{-1}$  is the acoustic attenuation length of a plane wave traveling in the duct,

$$\alpha_{\text{duct}} \approx \frac{z_{(0,n)}}{a_{\text{cavity}}} (\gamma - 1 + \sqrt{Pr}) \frac{\delta_T}{2a_{\text{duct}}} \quad . \quad (2)$$

The ducts perturb the eigenvalues by the fraction:

$$\left( \frac{\Delta z}{z} \right)_{(0,n)} = \sum_{\text{ducts}} \frac{a_{\text{duct}}^2}{4z_{(0,n)} a_{\text{cavity}}^2} \left[ i - (1+i) \frac{\xi \delta_T}{2a_{\text{duct}}} \right], \quad (3)$$

where the summation indicates separate terms are needed for the source and detector ducts.

Equations (1) - (3) show that reducing the radii of the ducts to reduce the perturbations  $(\Delta z/z)_{(0,n)}$  also reduces  $|p_{\text{det}}/p_s|$  and, consequently, the signal-to-noise ratio. Thus, the optimum values of the duct's radii will depend on the source's strength and detector's noise. Because the pre-factor in Eq. (1) contains  $a_s$  but not  $a_{\text{det}}$ , the optimization will result in  $a_s > a_{\text{det}}$ .

Equations (1) - (3) imply that we should choose the lengths  $l_{\text{trans-cavity}}$ ,  $l_{\text{terminal}}$ , and the radius of each duct to satisfy inequalities  $\alpha l_{\text{trans-cavity}} < 1$  and  $\alpha l_{\text{terminal}} > 1$ , so that the sound propagating from the source to the cavity and from the cavity to the detector is only weakly attenuated and the signal-to-noise ratio is only slightly reduced. Simultaneously, the much larger values of  $\alpha l_{\text{terminal}}$  would ensure that sound traveling in the terminal ducts is greatly attenuated and, thereby, ensure that high- $Q$  resonances do not occur in the

**Table 1.** Dimensions for acoustic models.

	Source	Detector
duct I.D. / mm	1.80	1.37
duct O.D. / mm	2.41	1.83
$l_{\text{trans-cavity}}$ / m	0.44	0.35
$l_{\text{terminal}}$ / m	1.71	1.71
$V_{\text{trans}}$ / mm <sup>3</sup>	11 <sup>a</sup>	8.8
$A_{\text{trans}}$ / mm <sup>2</sup>	140 <sup>a</sup>	60
$\alpha^{-1}$ / m; [700 K, 50 kPa, (0,3)]	0.15	0.11
$\alpha^{-1}$ / m; [273 K, 400 kPa, (0,2)]	0.95	0.73
$\delta_T / a_{\text{duct}}$ ; [700 K, 50 kPa, (0,2)]	0.14	0.18
$\delta_T / a_{\text{duct}}$ ; [273 K, 400 kPa, (0,5)]	0.016	0.021

<sup>a</sup>values for each of the two conical cavities in Fig. 3.

combined duct, provided that the transducers themselves do not reflect sound strongly.

We could only approximate the idealized {ducts + transducers} system because of practical constraints. For example, we minimized the volumes  $V_{\text{trans}}$  of the transducers in contact with the gas; however, the transducer volumes still generated significant reflections. Also,  $l_{\text{trans-cavity}}$  must be at least as long as the distance from the cavity to room temperature. Finally,  $\alpha^{-1}$  approaches 1 m at 400 kPa and 273 K (Table 1) making it difficult to achieve  $\alpha l_{\text{terminal}} \gg 1$  under all conditions.

We note that a commercially manufactured “probe” microphone that is designed to measure sound pressures in hostile environments, such as automobile exhaust systems, uses a system of duct, detector, and terminal duct resembling the one described here. [4]

Our system of {ducts + transducers} embodies several other design concepts that we briefly describe.

The extensions of the pressure vessel and the transducer housings protected the transducers from high temperatures and large differential pressures. The source and detector were in separate housings to minimize mechanical and electrical crosstalk between them. No crosstalk was detected.

As sketched in Fig. 1, separate ducts were used to flow gas into and out of the cavity. A small fraction of the gas ( $\approx 4\%$  for the source and  $\approx 1\%$  for the detector) flowed from the cavity through each acoustic

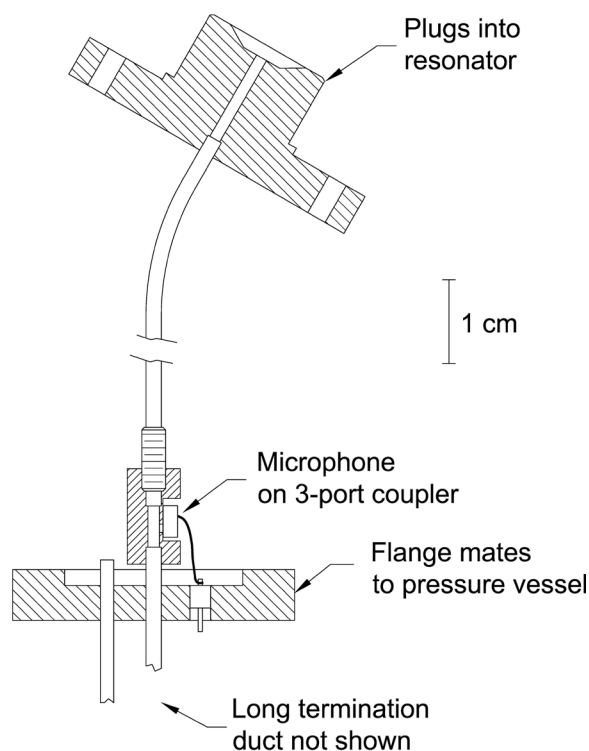


Figure 2. Detector transducer 3-port coupler and ducts.

duct assembly, and then back into the pressure vessel. This gas flow ensured that impurity gases originating in the transducers did not diffuse into the cavity.

The acoustic source had bilateral symmetry so that its center of mass did not move when it generated sound. We expected that this feature would reduce the coupling of the source’s motion to mechanical resonances in the cavity’s walls, the thermostat, etc.

The transducer housings were designed so that it was possible to replace either the source or the detector without disassembling the resonator, the main pressure vessel, or the thermostat.

The cavity of NIST’s acoustic thermometer is so nearly spherical that the (3,1) non-radial mode is well-separated from the (0,2) radial mode. [5,6] The additional perturbations from the acoustic ducts are smaller than the perturbations from the cavity’s imperfect shape. A new acoustic thermometer should follow the recommendation of Section 4.1 of Ref. [7] to join the acoustic ducts to the cavity at locations that minimize the detected amplitude of the (3,1) mode relative to the amplitude of the (0,2) mode.

## TRANSDUCERS AND DUCTS

### Detector Transducer

The detector transducer was a small, commercially-manufactured, microphone used in hand-held devices (Knowles Electronics<sup>1</sup>, SiSonic Model SPM0102NE3, www.knowles.com). The microphone had a built-in preamplifier that we powered with batteries (power dissipation  $\approx 0.5$  mW) located outside the transducer housing. A commercial lock-in amplifier operating in voltage mode measured the microphone’s output.

The microphone had the external dimensions  $4.72 \text{ mm} \times 3.76 \text{ mm} \times 1.50 \text{ mm}$ . It had a port  $0.84 \text{ mm}$  in diameter leading to the sensitive element. We disassembled a microphone and estimated its internal, gas-filled volume  $V_{\text{trans}} \approx 8.8 \text{ mm}^3$  and its internal surface area  $A_{\text{trans}} \approx 60 \text{ mm}^2$ . We used quick-setting epoxy to seal the detector transducer into a 3-port, custom-made, coupler. (The other ports accepted the duct and the terminal duct. See Fig. 2.)

The limited high-frequency response of the commercial microphone did not limit the data for the present acoustic thermometer because, above 10 kHz, resonances in the thermometer’s structure led to large errors in the determination of  $T - T_{90}$ .

<sup>1</sup> In order to describe materials and procedures adequately, it is occasionally necessary to identify commercial products by manufacturer’s name or label. In no instance does such identification imply endorsement by the National Institute of Standards and Technology, nor does it imply that the particular product or equipment is necessarily the best available for the purpose.

## Source Transducer

The acoustic source must: (1) generate a high sound pressure because of the large impedance mismatch between the ducts and the cavity, (2) have a small effective volume to minimize its perturbation of the cavity's resonances, (3) dissipate little power, and (4) have only a weak mechanical coupling to the solid components of the acoustic thermometer. Lin *et al* achieved many of these objectives using piezoelectric ceramic transducers. [8] We adopted their transducer scheme when we developed the home-made acoustic source shown in the assembly drawing in Fig. 3.

The source contains two identical, bending-mode, lead-zirconate-titanate (PZT), piezoelectric transducers that were purchased from Piezo-Kinetics<sup>1</sup>. (Part number: ND-0.250-0.000-0.020-402 with tab; PKI-402 0.25" O.D.×0.020" thick) The PZTs faced each other on opposite sides of a 4-port coupler. (Two ports opened to the PZTs; one port opened to the source duct, and one opened to source's terminal duct.) The PZTs were driven by the same voltage and phased so that when the PZTs moved, their center of mass did not move. This symmetry minimized the coupling of the transverse motions of the PZTs to the solid components of the acoustic thermometer.

Each PZT had an outer diameter of 6.55 mm, a thickness of 0.51 mm, and was coated with a "wrap-around" electrode so that wires could be soldered to both electrodes on the same side of the disk. The PZTs were epoxied to the center of a roughened brass disk

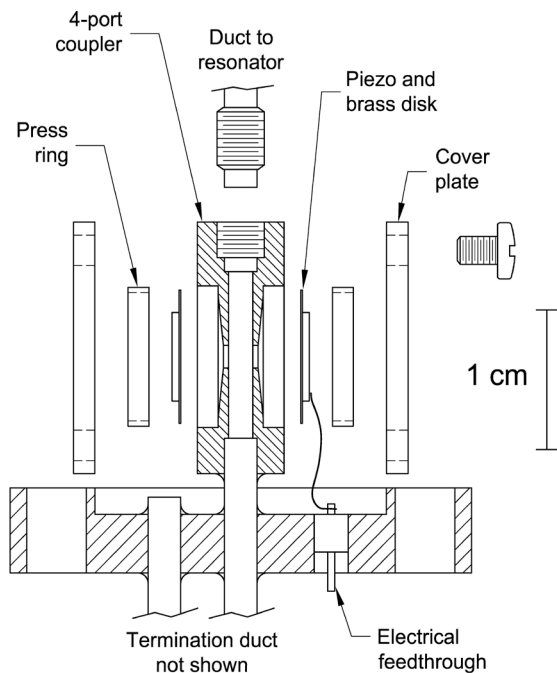


**Figure 3.** Exploded diagram of the source 4-port coupler, transducers, and attached ducts.

[diameter = 9.52 mm; thickness = 0.127 mm] that supported the PZTs in the coupler. Each brass disk was pressed against the body of the coupler by a stainless steel ring secured by a brass cover plate.

The PZT assembly had a resonance near 8.5 kHz with a full width at half maximum of 160 Hz. If we had used thicker disks, this resonance frequency would have been higher.

The source transducer was not designed to sustain differential pressures; therefore, it did not contain hermetic seals. However, the cover plates fit on the body of the coupler sufficiently well that sound transmission from the PZTs into the pressure vessel did not cause noticeable problems.

A shallow cone (half-angle = 84°) was machined out of each side of the coupler facing a PZT, leaving a gas-filled, conical, 11 mm<sup>3</sup> volume with a 0.47 mm wide gap between the center of the brass disk and the coupler. Because this gap was much wider than  $\delta_r$  and  $\delta_v$ , the attenuation of the gas motion within the coupler was not excessive. (In argon at 273 K, 2.5 kHz, and 50 kPa,  $\delta_r \approx 68 \mu\text{m}$  and  $\delta_v \approx 55 \mu\text{m}$ .) A deeper cone would have left a larger gas-filled volume that would generate larger temperature-dependent perturbations to the cavity's resonance frequencies. The surface area of each conical volume and brass disk was 140 mm<sup>2</sup>. A 1.63 mm diameter hole through the 4-port coupler connected each conical volume to the source duct and to the source-terminal duct.

An audio amplifier drove the PZT transducers with a maximum voltage of 30 V<sub>RMS</sub>. At this voltage, the heat generated within the PZTs did not damage the epoxy bonds to the brass disks. The driving voltage was reduced to as low as 0.6 V<sub>RMS</sub> at frequencies near the source resonance and pressures above 100 kPa to reduce stress on the epoxy bonds. Occasionally, at pressures below 100 kPa, we observed hysteresis of the measured acoustic resonances slightly larger than the noise. We do not know if this effect is due to transducer heating or to changes in the piezo/disk compliance following a change in frequency.

## Ducts

The duct leading from the cavity resonator to the 3-port coupler (and the detector transducer) was stainless-steel "regular wall" hypodermic tubing with the nominal dimensions 1.83 mm O.D., 1.37 mm I.D., and 34.7 cm long. To model this duct, we estimated that 22.6 cm of its length was isothermal at the temperature of the cavity, 6.6 cm was in a linear temperature gradient, and 5.5 cm was at room temperature. The termination duct from the 3-port coupler was made from the same 1.83 mm O.D. tubing and was 1.71 m long.

The duct leading from the cavity to the 4-port coupler (and the source transducers) was also stainless-steel “regular wall” hypodermic tubing with the nominal dimensions 2.41 mm O.D., 1.80 mm I.D., and 43.7 cm long. We estimated that 31.6 cm of its length was isothermal at the temperature of the cavity, 6.6 cm was in a linear temperature gradient, and 5.5 cm was at room temperature. The termination duct was made from the same tubing and was 1.71 m long.

The tubes were annealed to facilitate bending them near the cavity and also bending the termination duct into a coil approximately 10 cm in diameter.

In developing the system {ducts + transducers}, we retrofit the ducts into an earlier version of NIST’s acoustic thermometer. The thermometer had two available extensions of the pressure vessel with slightly different inner diameters. Consequently, we optimized  $a_s$  and  $a_{det}$  within the constraint of the available space. We chose different lengths for the source and detector ducts so that the maximum perturbations from these ducts would occur at different frequencies.

After assembly of the thermometer, we added elastomer dampers onto the room temperature portions of the ducts. These dampers reduced low-frequency noise due to vibrations and improved the signal-to-noise of our measurements.

## Transducer Housings

The terminal ducts are open to the transducer housings. For modeling, we approximated the source-transducer housing by a volume of 5 cm<sup>3</sup> and the detector-transducer housing by a volume of 4 cm<sup>3</sup>. The calculated perturbations are only weakly sensitive to these volumes and weakly sensitive to the tubes connecting the housings to the pressure vessel.

## CALCULATED PERTURBATIONS

### Isothermal Model

Gillis et al. used a coupled waveguide model to calculate perturbations  $\Delta F_{(0,n)}$  of the complex resonance frequency  $F_{(0,n)} \equiv f_{(0,n)} + ig_{(0,n)}$  for our cavity at 273 K (Section 3.5 of [3]). Figure 4 plots the results of the same calculation at 293 K using the dimensions listed in Table 1 for the {transducer + duct} systems.

Figure 4 has two horizontal scales: a frequency ( $f$ ) scale and a wavenumber scale  $(ka)_{cavity}$ . Here,  $a$  is the radius of the cavity and  $k \equiv 2\pi f/c$ , where  $f$  is the frequency at which the source is operated, and  $c$  is the speed of sound in the cavity. The values of  $ka$  for the radially-symmetric  $(0,n)$  resonances of the cavity are indicated by arrows in Fig. 4 and are insensitive to the

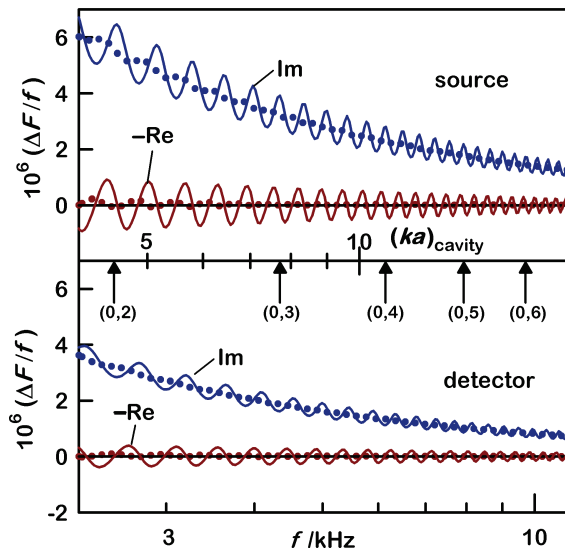


**Figure 4.** Fractional perturbations generated by the source (top) and detector (bottom) to the complex resonance frequencies of an argon-filled spherical cavity at 293 K for two argon pressures: 50 kPa (dotted curves) and 400 kPa (solid curves). The scale between the two panels is the product of the acoustic wavenumber  $k$  and the cavity radius  $a$ . The arrows indicate the values of  $(ka)_{cavity}$  for the radial modes  $(0,2)$ ,  $(0,3)$ , etc.

cavity’s temperature even though the resonance frequencies are temperature-dependent.

As shown in Fig. 4, both the real part (frequency shift,  $\text{Re}$ ) and the imaginary part (half-width increase,  $\text{Im}$ ) of the perturbations are oscillatory functions of  $(ka)_{cavity}$ . These oscillations result from reflections of sound at the transducers; therefore, the period of the oscillations is determined by the effective lengths of the ducts  $l_{trans-cavity}$ . The effective lengths are sensitive to details of the duct geometry, and, as discussed in the next section, the temperature distribution along the ducts. The oscillations shift significantly with small variations in effective length. However, prediction of the exact frequency dependence of the oscillations is not required if we take the amplitude of the oscillations of  $\text{Re}(\Delta F_{(0,n)})$  as a reasonable estimate for the upper bound of the frequency perturbation.

At 293 K, the largest value of  $\text{Re}(\Delta F_{(0,n)})$  from the source duct is  $0.85 \times 10^{-6} f_{(0,2)}$  for the  $(0,2)$  mode at 400 kPa, which corresponds to 0.85 mK at 500 K. The perturbations are smaller at lower pressures and for the higher-frequency modes. Under similar conditions, the largest values of  $\text{Re}(\Delta F_{(0,n)})$  for the detector duct are less than half the values for the source duct.

### Effects of Temperature Changes

We consider three effects that occur when the furnace’s temperature is increased from 293 K to

700 K at constant pressure: (1) the speed of sound in argon in the cavity and the heated sections of the ducts increases by the factor  $(700/293)^{1/2} \approx 1.5$ , (2) the density of the argon in the heated volume decreases by the factor  $(293/700) \approx 0.42$ , and (3) a temperature gradient from 293 K to 700 K is created along approximately 6.6 cm of each duct.

The increase of the speed-of-sound increases the resonance frequencies of the cavity by the factor  $\approx 1.5$ ; however, ignoring thermal expansion, the value of  $k_{\text{cavity}}$  is unchanged. The wavenumber in the room-temperature portion of each duct  $k_{\text{ducts}}$  increases by the same factor  $\approx 1.5$ , thereby decreasing the effective length of each duct. We estimate the decrease for the source duct is from 43.7 cm to 38.6 cm and for the detector from 34.7 cm to 29.6. The smaller effective lengths increase the period of the oscillations in Fig. 4.

For each  $(0,n)$  mode, the decrease of density of the argon and the frequency increase combine to decrease the plane-wave attenuation-lengths  $\alpha^{-1}$  by the factor 0.58 in the hot portion of each duct. This reduces the signal-to-noise ratios and the amplitudes of the frequency perturbations.

When the gas in a duct sustains a temperature difference over the length  $l_{\text{grad}}$ , the change in its density and the speed of sound will reflect sound. In low-density argon, a temperature change from 293 K to 700 K in the distance  $l_{\text{grad}} \ll 1/k$  generates a pressure-reflection coefficient with magnitude 0.21. [9] In the regime  $kl_{\text{grad}} \gg 1$ , the reflection coefficient varies as  $0.18/kl_{\text{grad}}$ . For NIST's acoustic thermometer,  $l_{\text{grad}} \approx 6.6$  cm and  $k_{(0,2)} = 0.505$  cm $^{-1}$ . Therefore, the reflection coefficient for the  $(0,2)$  mode has the magnitude 0.05 and it is smaller for the other modes.

## PERFORMANCE TESTS

We conducted two types of performance tests of the system {ducts + transducers}.

First, while the resonator was filled with argon at 100 kPa and in a partially assembled configuration at room temperature, we gradually heated to 470 K almost the entire lengths of either the detector termination duct, the source termination duct, or the source-to-cavity duct, while repeatedly measuring the frequencies  $f_{(0,2)}$ ,  $f_{(0,3)}$ ,  $f_{(0,4)}$ , and  $f_{(0,5)}$ . We fitted frequency ratios such as  $R_{3,2} \equiv f_{(0,3)}/f_{(0,2)}$  to linear functions of the duct's nominal temperature. For the most sensitive source-to-cavity duct, the fractional changes in the ratios were:  $10^6 \Delta R_{3,2}/R_{3,2} = -0.01 \pm 0.61$ ,  $10^6 \Delta R_{4,2}/R_{4,2} = -0.54 \pm 0.87$ , and  $10^6 \Delta R_{5,2}/R_{5,2} = 0.94 \pm 1.00$  between room temperature and 470 K. (Here and below, the uncertainties are one standard uncertainty.) Thus, the ratios of the  $(0,n)$  resonance frequencies were independent of the

temperature of the ducts within the noise of the tests. During the same tests, the scaled half-widths of the resonances  $10^6 g_{(0,n)}/f_{(0,n)}$  increased by  $1.46 \pm 0.50$ ,  $0.92 \pm 0.71$ ,  $1.85 \pm 0.90$ , and  $3.02 \pm 1.20$  for the  $(0,2)$ ,  $(0,3)$ ,  $(0,4)$  and  $(0,5)$  modes, respectively. Heating of the duct in the test configuration caused temperature inhomogeneities in the gas in the cavity that do not occur during normal operation with the thermostat fully assembled. The observed increases in  $g_{(0,n)}$  are consistent with a simple model of thermal gradients driven by localized heating of the cavity wall.

Second, we looked for possible dependences of the  $f_{(0,n)}$  and  $g_{(0,n)}$  on the voltage applied to the acoustic source. We conducted this test at 289 K and 200 kPa by measuring the complex resonance frequency  $F_{(0,n)} \equiv f_{(0,n)} + ig_{(0,n)}$  of the  $(0,2)$ ,  $(0,3)$ ,  $(0,4)$ , and  $(0,5)$  modes with the usual drive voltage  $V_S$  and also with the voltages  $V = 2V_S$  and  $4V_S$ . We fitted the results by the function  $F_{(0,n)} = F_{(0,n)}(0)[1 + (a + ib)V/V_S]$  to obtain the values  $10^6 a = 0.09 \pm 0.23$  and  $10^6 b = 0.02 \pm 0.23$ , which are zero within the uncertainties. We also fitted the results by the quadratic function of  $(V/V_S)^2$ :  $F_{(0,n)} = F_{(0,n)}(0)[1 + (a + ib)(V/V_S)^2]$  and obtained values of  $a$  and  $b$  that were zero within the uncertainties.

## ACKNOWLEDGEMENT

We thank Wyatt Miller for assistance in fabricating parts, assembling the thermometer and conducting test measurements.

## REFERENCES

- 1 Fischer, J., de Podesta, M., Hill, K. D., Moldover, M. R., Pitre, L., Rusby, R., Steur, P., Tamura, O., White, R., and Wolber, L., *Int. J. Thermophysics*, **32**, 12-25 (2011) and references therein.
- 2 Ripple D. C., Strouse G. F., Moldover M. R., *Int. J. Thermophysics*, **28**, 1789-1799 (2007).
- 3 Gillis, K. A., H. Lin, and M. R. Moldover, *J. Res. Natl. Inst. Stand. Technol.* **114**, 263-285 (2009)
- 4 Brüel & Kjør Sound & Vibration Measurement A/S Skodsborgvej, Denmark; Probe Microphone Type 4182.
- 5 Ripple, D. C., Defibaugh, D. R., Moldover, M. R. and Strouse, G.F., in *TEMPERATURE: Its Measurement and Control in Science and Industry; Vol. 7*, edited by D.C. Ripple et al., AIP Conference Proceedings 684, American Institute of Physics, Melville, NY, 2003, pp. 25-30.
- 6 Moldover, M.R., Trusler, J.P.M, Edwards, T.J., Mehl, J.B. and Davis, R.S., *J. Res of NBS*, **93**, 85-144 (1988).
- 7 Mehl, J. B., Moldover, M. R. and Pitre, L., *Metrologia*, **41**, 295-304 (2004).
- 8 Lin, H, Gillis, K.A., Zhang, J.T., *Int. J. Thermophysics*, **31**, 1234-47 (2010).
- 9 K. A. Gillis, unpublished